Experimental investigation of thrust vectoring by flow separation control on a rectangular M = 1.45 jet

VINCENT JAUNET, ERWAN COLLIN,
ANTON LEBEDEV, CARINE FOURMENT
LABORATOIRE D'ETUDES AÉRODYNAMIQUES
UNIVERSITÉ DE POITIERS, ENSMA, CNRS
LEA/CEAT 43 ROUTE DE L'AÉRODROME
86000 POITIERS, FRANCE

Abstract :

A crossflow jet actuator is used on the smallest dimension of the exhaust of a rectangular nozzle. By this way separation is introduced, creating asymetry and vectorizing the main flow. PIV measurements were performed for several fluidic injection rates. Effects of the manipulation on the main flow are discussed.

Résumé :

La vectorisation d'un jet supersonique rectangulaire est obtenue par soufflage à contre-courant sur la petite dimension de le section de sortie de la tuyère. Un décollement est ainsi créé, dissymétrisant l'écoulement. Des mesures PIV ont été effectuées montrant l'influence du contrôle sur le jet principal.

1 Introduction

A fundamental issue regarding the performance of any military aircraft is maneuvrability and thrust vectoring is a very efficient way to improve aircraft's motion abilities. First generation of thrust vectoring nozzle deflected the engine's exhaust through mechanical actuactors. Those kind of nozzles, even very efficient, need addition of hydraulic and mechanical actuators, increasing by the way the aircraft's weight, production and maintenance costs. Thus an alternative solution is the fluidic thrust vectoring : secondary air streams are used to vectorized the primary jet. Such techniques are expected to reduce nozzle weight up to 80% and maintenance cost up to 50% [3]. Thus many fluidic thrust vectoring were developped such as *counterflow thrust vectoring* [8, 10, 11] in which a counterflow shear created between the primary jet and an aditional exhaust collar redirect the jet ; or *secondary injection thrust vectoring* [3, 13] in which a secondary jet is introduced into the supersonic primary jet, creating a shock wave and causing assymetry in the flow field and unbalancing lateral forces on the nozzle. Synthetic jets can also be used to vector jets [9], vectorization is then obtain by interaction between the synthetic jet and the primary one, creating asymetric pressure field in the main flow.

As the *secondary injection thrust vectoring* technique, the one used in this study utilizes a secondary jet in the nozzle. The main difference is that the injection occures at the exhaust section of the nozzle on an additional small divergent (*Fig. :* 1). The role of this divergent is to decrease the energy needed to make the boundary layer detach from wall, and then vectorizing the primary jet more easily. With this method, there is no need of external mechanical apparatus and the injection mass flow rate stays in reasonable proportions, thus integrating this actuator on an aircraft seems workable.

Both subsonic [6, 12] and supersonic [1, 2, 5, 14] rectangular jets have already been describred in literature, showing different behaviours depending on the nozzle aspect ratio and inlet flow conditions. The jet used in this study is supersonic and exits from a particular rectangular nozzle : the actuator added at the exhaust of the nozzle impose a centered expansion fan (*Fig. :* 6). Thus the jet cannot be regularly expanded around the whole nozzle, and its shock structure is modified accordingly. This makes the jet studied here different from other experimentations.Furthermore, vectorizing the main jet creates additional shock and expansion fan, leading to a really complex asymetric flow.

2 Apparatus, Instrumentation

2.1 Experimental device

Experiments were conducted in the S150HP blow-down facility (Centre d'Etudes Aérodynamiques et Thermiques at Poitiers (France)), using dry air compressed up to 200 bars and stored in large tanks.
The blow-down facility was fitted with a rectangular nozzle having an aspect ratio of $5:1$. The dimension of

the exhaust section is heigth $l = 150$ mm and width $h = 30$ mm. The jet is exiting in a square shaped test section of 500 mm wide.
The test section was supplied with ambiant air through a 1 m^2 square shaped convergent.
The Reynolds number of the jet, based on the mean axial velocity ($380\ m.s^{-1}$) at the center of the jet and the hydraulic diameter of the exhaust section D_h [1] is equal to $3.3 \cdot 10^6$.

The exhaust section of the nozzle was fitted with 2 divergents on its smallest dimension. Those divergents are 30 mm long and sloping down with an angle of $10\,^\circ$ from the main flow. Furthermore, a thin crossflow jet (0.5 mm wide) was implanted in one of the divergents and occupied the whole width of the nozzle. This actuator blew out oposite to the main flow with an angle of $45\,^\circ$. Several fluidic injection rate[2] ΔQ were imposed from 0 to 1.62 with fixed stagnation conditions.

Stagnation pressure was chosen equal to 3.7 bar, which is the minimum pressure avoiding detachement before the end of the nozzle, and maintained steady by an hydraulic valve and kept at its nominal value within variations of ± 0.05 bar. Stagnation temperature was measured during all the experimentations. It could vary from $250\,^\circ$K up to $260\,^\circ$K from one experiment to another (depending mainly on the atmospheric conditions and tank pressure). This leads to less than 2 % of variation on the jet speed.
A cartesian coordinate system {x, y, z} was chosen with its origin placed at the center of the exhaust section of the main jet and with the x-axis along the streamwise direction and the y-axis and z-axis along the long and short dimensions of the nozzle.

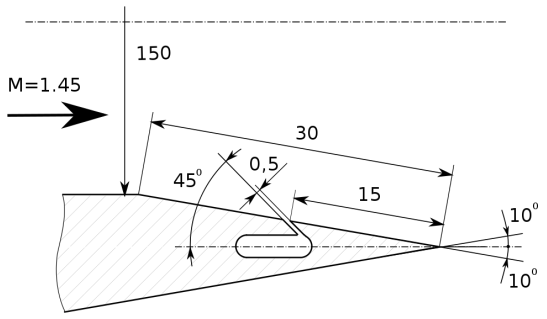

Figure 1: Divergent and actuator

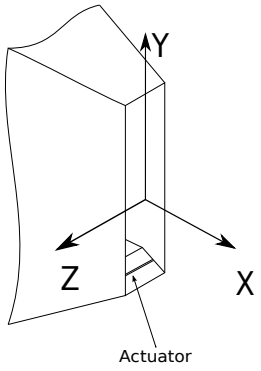

Figure 2: Chosen coordinate system and localisation of the actuator

Distances were adimensionalised by the small dimension of the nozzle h and were noted x^*, y^* and z^*. Flow speed magnitude U was adimensionalised, and noted U^*, by the jet speed magnitude at the center of the exhaust section U_1 and the external flow speed magnitude at the same {x, z} location U_2 :

$$U^* = \frac{U - U_2}{U_1 - U_2}$$

Then dimensionless velocity components (V_x^*, V_y^*) were calculated :

$$\alpha = atan(\frac{V_y}{V_x})\ ;\ V_x^* = U^* cos(\alpha)\ ;\ V_y^* = U^* sin(\alpha)$$

2.2 Measurement devices

Particule Image Velocimetry measurements were performed in {x, y} planes for several distances from the centerline and different fluidic injection rates. Flow xas seeded with $Si0_2$ particules, which mean diameter is less than $1\mu m$. 200 pairs of images were taken for each configuration.
The PIV device used in this study was a 1376×1040 pixels CCD camera equiped with an 28 mm objective and

[1] $D_h = \frac{4(l \times h)}{2(l + h)}$
[2] $\Delta Q = \frac{Q_{injected}}{Q_{nozzle}} \times 100$

two 190mJ Nd-YAG laser cavities. The time between each laser pulse was imposed at 5 μs which corresponds to a particule displacement of 7 pixels. Image processing was conducted by the *LaVision* software. First, average of each set of images is calculated and substracted to each image in order to remove blur and background noise. In a second time, the instantaneous velocity fields were calculated using a correlation computed with standard FFT. Interogation window size started at 64×64 pixels with an overlap of 50% and the final pass was conducted with a 16×16 pixels window overlapped also at 50 %. Finaly, spurious vectors were corrected using the *Gappy POD* method [4, 7].

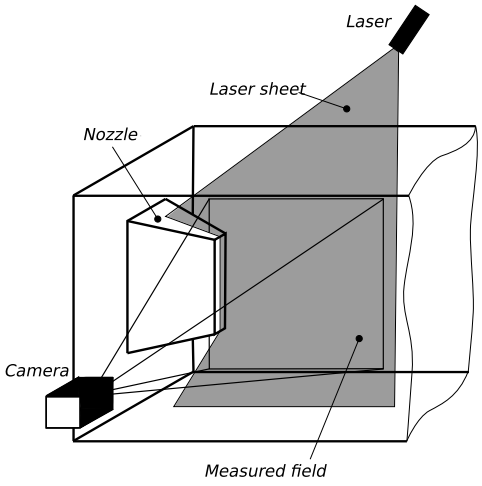

Figure 3: PIV measurement

3 Results and Discussions

3.1 Non-manipulated jet

Mean axial velocity measured by PIV are given in *Fig. :* 7.
Firstly, Mach number is not the same at the whole exhaust section of the nozzle (*Fig. :* 6). consequently, the adaptation conditions and the strengh of the adaptation shock are not equal over the exhaust section. Furthermore, the centered expansion fan created by the actuator interacts with the adaptation shock and makes it curve. It is interesting to notice that the first detachement line position seems to be located on the divergent and does not move more upwind in the nozzle.
Secondly, in order to give a better interpretation of the PIV results, the flow must be considered as a three-dimensional one as soon as it leaves the nozzle. The acceleration observed at $x^* = 3.5$ (*Fig. :* 5), also observed in [1] is due to expansions in $\{y, z\}$ planes accelerating the flow by more than 20 %.
All these effects make the interpretation of the PIV results (*Fig. :* 7) quite difficult, even in the non-maniplated case $\Delta Q = 0\%$.

3.2 Vectorization

Vectorization is controlled varying the pressure in the actuator plenum chamber, then a shock is created from the inside of the nozzle getting stronger with increasing pressure injection. This shock is related to a boundary layer detachement which oblies the flow to change direction. This shock is then followed by an expansion fan and a readaptation shock (*Fig. :* 6).
The flow structure is completely disorganized by the secondary injection (*Fig. :* 7), shock-expansion network becomes asymetric and the boundaries of the jet move in opposite direction of the injection.
Two different regimes can be obserbed by increasing injection pressure. One is for low injection pressure $\Delta Q < 1.0$ %, and for $\Delta Q > 1.0$ % the detachement shock impiges the opposite nozzle edge, probably displacing the sonic line from the nozzle throat to another location near the exhaust section of the nozzle. Nevertheless, this regime seems to be more efficient than the first one.

Vertical velocity profiles at $z^* = 0$ nearby the exhaust section (*Fig. :* 4) permits the location of the detachement shock, thus vectorization mechanism can be determined. For $\Delta Q < 1.0$ % vertical velocity is increased in the part of the flow under the shock, other parts of the jet do not seem to be modified. For higher injection rates the whole profile is modified and the vertical velocity is getting higher as the injection rate increases. According to these observations, the vectorization mechanism is related to a shock mechanism constraining the flow to change direction.

4 Concluding remarks

Two different regimes of vectorization are observed studying this actuator. The first one, occuring for low fluidic injection rates, seems to be related to shock-deviation mechanism. An important observation is that the vectorization seems progressive, this is essential for industrial implementations. Furthermore, the jet deviation created by this regime seems more important than what it could be expected by addition of flaps at the exhaust section of the nozzle. On the other side, the second regime, for highest injection rates, is characterized by modification of the entire flow, even inside of the nozzle. Nevertheless, it seems more efficient than the first one.
This study also highlights the importance of three-dimensional effects on the organisation of the mean flow. Thus, mixing layers and turbulence are also expected to be affected by 3D effects. Future experiments will permit to observe ans quantify these modifications.
Vectorization of the main jet is complex because of the nozzle geometry and especially the fact the actuation is performed on its smallest dimension. Moreover, actuator design influence was not discussed in this study and the one designed for this experiment is probably not the more efficient in terms of thrust-vector angle.

5 Figures

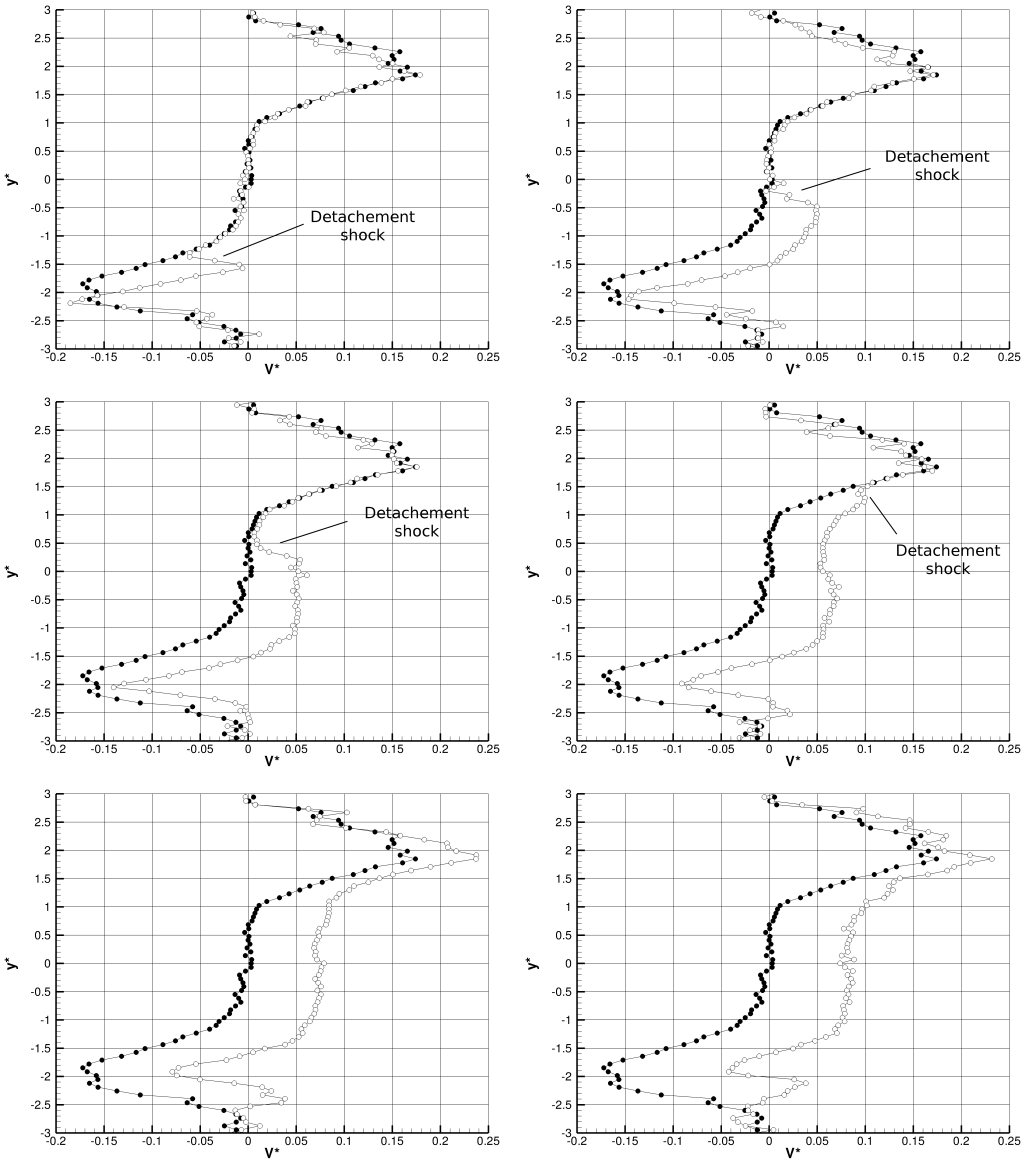

Figure 4: Vertical component of velocity V^* profiles at $(x^*, z^*) = (0.4, 0)$. ●: Unmanipulated case, ○: vectorized cases (from top to bottom and left to right : $\Delta Q = 0.31\%$, $\Delta Q = 0.63\%$, $\Delta Q = 0.78\%$, $\Delta Q = 1.0\%$, $\Delta Q = 1.3\%$, $\Delta Q = 1.62\%$)

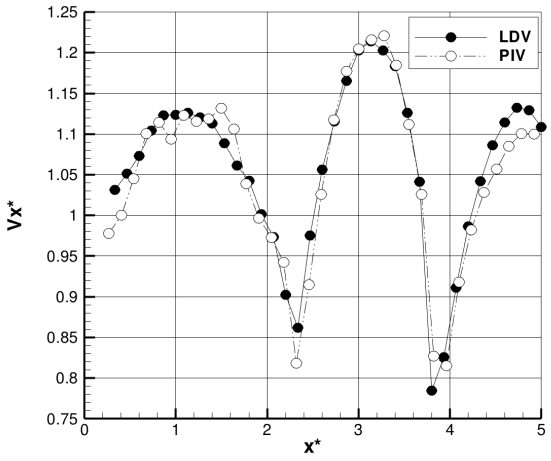

Figure 5: Comparison of mean axial velocity on the centerline of the jet measured with PIV and LDV

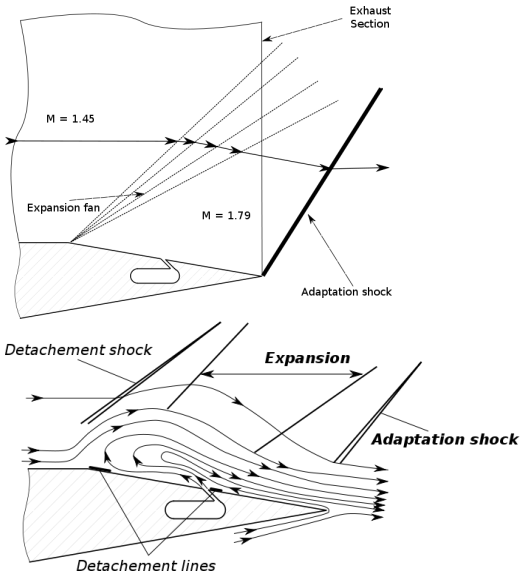

Figure 6: Topology of the flow on the divergent.Top : unmanipulated case, bottom : manipulated case

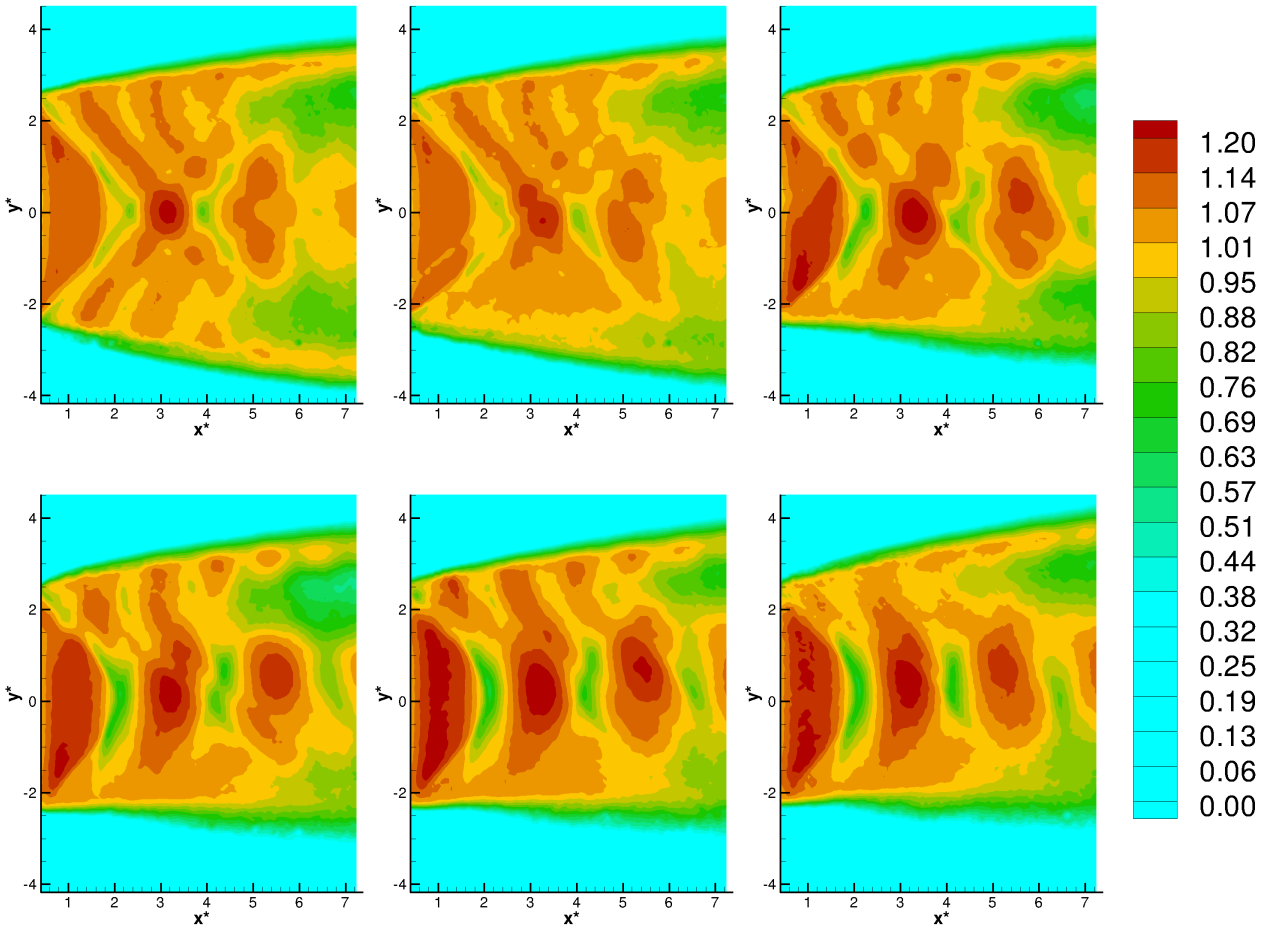

Figure 7: Iso-contours of of mean axial velocity U^* downstream of the nozzle, from left to right and top to bottom : $\Delta Q = 0\%$, $\Delta Q = 0.31\%$, $\Delta Q = 0.63\%$, $\Delta Q = 1.0\%$, $\Delta Q = 1.3\%$, $\Delta Q = 1.62\%$

Acknowledgments

The authors wich to thank the french ministery of defense and the Region Poitou-Charentes for suporting this study.

References

[1] M. B. Alkislar. Flow field measurements in a screeching rectangular jet, 2001.

[2] M.B. Alkislar, A. Krothapalli, and L. M. Lourenco. Structure of a screeching rectangular jet : a stereoscopic particule image velocimetry study. *JFM*, 489:121–154, 2003.

[3] K.A. Deere et al. Computational study of fluidic thrust vectoring using separation control in a nozzle. *21st AIAA Applied Aerodynamics Conference*, 2003.

[4] R. Everson and L. Sirovich. Karhunen-loève procedure for gappy data. *J. Opt.Soc.Am. A, vol. 12, No. 8*, 1995.

[5] E. Gutmark, K. C. Schadow, and C. J. Bicker. Near acoustique field and schock structure of rectangular jets. *AIAA Journal*, 28:1163–1170, 1990.

[6] A. Krothapalli, D. Baganoff, and K. Karamcheti. On the mixing of a rectangular jet. *JFM*, 107:201–220, 1981.

[7] N. Murray and L. Ukeiley. An application of gappy pod. *Exp. Fluids, 42:79-91*, 2007.

[8] M.M. Santos. *Experimental study on counter flow thrust vectoring of a gaz turbine engine*. PhD thesis, Florida State University, 2005.

[9] B.L. Smith and A. Glezer. Jet vectoring using synthetic jets. *JFM*, 458:1–34, 2002.

[10] P.J. Strykowski and A. Krothapalli. The countercurrent mixing layer : strategies for shear layer control. *AIAA 93-3260*, 1993.

[11] P.J. Strykowski and A. Krothapalli. Enhancement of mixing in high-speed heated jet using a counterflow nozzle. *AIAA Journal Vol. 31, number 11*, 1993.

[12] Y. Tsuchiya and C. Horikoshi. On the spread of a rectangular jets. *Exp. in fluids*, 4:197–204, 1986.

[13] C.C. Wu. A computational study of secondary injection thrust vector control. *AIAA 95-1787*, 1995.

[14] K. B. M. Q. Zaman. Axis swithching and spreading of an asymetric jet : the role of coherent structure dynamcis. *JFM*, 316:1–27, 1996.